Bank strength variability and its impact on the system-scale morphodynamics of the upper Amazon River in Brazil

Muriel Z.M. Brückner[1,2], Rolf E. Aalto[1,3], Jim Best[4], Renato Paes de Almeida[5], Andrew P. Nicholas[1], Philip J. Ashworth[6], Marco Ianniruberto[7]

[1]*Department of Geography, Faculty of Environment, Science and Economy, University of Exeter, Exeter, UK*

[2] *now at: Department of Civil and Environmental Engineering, Louisiana State University, Baton Rouge, USA*

[3]*Department of Earth and Space Sciences, University of Washington, Seattle, USA.*

[4]*Departments of Earth Sciences and Environmental Change, Geography & GIS, Mechanical Science & Engineering, and Ven Te Chow Hydrosystems Laboratory, University of Illinois at Urbana-Champaign, Urbana, USA*

[5]*Department of Sedimentary and Environmental Geology, University of São Paulo, São Paulo, Brazil*

[6]*School of Applied Sciences, University of Brighton, Brighton, UK*

[7]*Department of Geosciences, University of Brasília, Brasília, Brazil*

ABSTRACT

Large anabranching rivers form channels in sediments of varying strength, resulting from erosional and depositional processes that act over geological timescales. Although bank strength variability is known to affect channel morphodynamics, its impact on the migration of large sand bed rivers remains poorly understood. We report the first in-situ measurements of bank strength from a ~100 km long reach of the Solimões River, the Brazilian Amazon River upstream of

Manaus. These show that cohesive muds in Pleistocene terraces along the river’s right margin have bank strengths up to three times greater than Holocene floodplain deposits comprising the left bank. Image analysis suggests these resistant outcrops determine channel-bar dynamics: channel widening and bar deposition are inhibited, which lowers planform curvature and reduces erosion of the opposing bank. Planform analysis of the 1,600 km long Solimões River between 1984-2021 shows that where the channel is associated with Pleistocene terraces, lower rates of bank erosion and bar deposition are evident. Heterogeneity in bank strength is thus a first-order control on the large-scale morphodynamics of the world’s largest lowland river.

INTRODUCTION

Large lowland sand-bed rivers develop anabranching channel patterns through the lateral migration of sinuous channels (Latrubesse, 2008). Migration is driven by morphodynamic feedbacks, whereby lateral erosion facilitates bar formation when channels widen (bank-pull), which encourages steering of the flow toward the outer bank, promoting bank erosion (bar-push) (Ashworth et al., 2000; Parker et al., 2011). These feedbacks depend on the morphological and associated hydraulic characteristics (planform curvature, flow direction, bed topography) and local bank strength, the latter controlling sediment resuspension and bank failure (Ashworth and Lewin, 2012; Zhao et al., 2022). River bank strength may be highly variable, and is a function of local stratigraphy and sediment composition, grain size, diagenesis and vegetation (Darby and Thorne, 1996; Motta et al., 2012). Although such variability controls local and reach-scale migration dynamics (Güneralp and Rhoads, 2011; Schwendel et al., 2015), studies have been limited to smaller single-threaded rivers, despite longstanding evidence that topographic and lithological variability are controls on many large rivers (Potter, 1978).

The Amazon River occupies a 100,000 km^2 wide Holocene floodplain incised into Late Tertiary and Quaternary deposits (Mertes and Dunne, 2022). In central Amazonia, the interfluves between major rivers comprise fluvial deposits formed at a higher base level than the modern alluvial plain, originally mapped as the Içá Formation (Maia et al., 1977), and later revealed as Late Pleistocene in age (Rossetti et al., 2015; Pupim et al., 2019). Such Pleistocene cohesive and cemented sediments (PCCS) form terraces tens of meters in elevation that comprise weakly consolidated fine to coarse sand-, silt-, and mudstones (Rossetti et al., 2015; Mertes and Dunne, 2022). Due to Holocene river incision, the active channel now frequently flows against, and along, these terraces. The Solimões River, the Brazilian Amazon River upstream of Manaus, has an anabranching channel belt that transitions from high sinuosity (1.6) to low sinuosity (1.1) around the confluence with the Japurá River (Mertes et al., 1996), accompanied by varying migration rates along both banks (Figure 1A). This transition has been linked to changes in slope, underlying geology, and floodplain narrowing caused by older terraces (Mertes et al., 1996; Mertes and Dunne, 2022). However, these previous studies provided neither measurements nor detailed planform analyses. Herein, we hypothesize that PCCS possess a higher bank strength than Holocene alluvium and that this difference controls larger scale river morphology and dynamics. We provide the first in-situ measurements of bank strength along the Solimões River and compare these to reach-scale morphodynamics from remotely sensed data. We quantify bank erosion and deposition rates along the entire Solimões River, demonstrate their dependence on the proximity of the river to PCCS, and provide a mechanistic explanation for how variability in bank strength exerts a first-order control on the migration behavior of one of the world's largest anabranching rivers.

METHODS

We briefly describe the methodology below, with more details provided in the Supplementary Materials (SM[1]).

Field Data from the Solimões River

We collected 210 measurements of bank strength (Figure 2) using a hand-held Pilcon shear vane and a cohesion strength meter (Mark III) at 30 locations along a 100-km reach of the Solimões River that has experienced contrasting erosion between its south (right bank looking downstream) and north (left looking downstream) banks since 1967 (Figure 1A). The shear vane (SV) records the axial strength of the top layer (He et al., 2018), whereas the cohesion strength meter (CSM) provides a critical shear stress for erosion based on a jet-pressure test (Tolhurst et al., 1999). To determine the morphology of submerged PCCS, we collected multibeam echo sounder (MBES) and side-scan sonar data for the near-bank channel bed in October 2022 (low flow stage). Side-scan return intensity data were overlain onto the processed MBES data that were gridded at 0.25 m (see SM[1]).

Image and GIS Analyses

We digitized Corona imagery from December 11th 1967 (USGS; *c.* 2m resolution) and extracted bank and bar lines to compare with Planet CubeSat data from October 2021 (*c.* 3 m resolution; Planet, 2023). To quantify channel migration, we produced four-year composite images (1984-1988 and 2019-2023; Boothroyd et al., 2021) to classify water and land masks from Landsat imagery (see SM[1]) in three reaches along the Solimões River (Figure 3A). These were classified as: i) freely meandering (reach I), ii) partially-constrained by PCCS (reach II), and iii) partially-constrained at the confluence with a secondary channel (reach III) based on FABDEM data (Hawker et al., 2022; see SM[1]). In addition, we computed channel centerlines based on banklines

(RivMap toolbox; Schwenk et al., 2017) to calculate channel sinuosity and mean annual erosion and deposition rates along each bank in 20- or 10-km segments based on the river kilometers given in nautical charts (Brazilian Navy 2001).

For the 1,600 km length of the Solimões River, the proximity of the bankline to PCCS terraces was measured at the scale of 10-km segments using FABDEM (Hawker et al., 2022), by measuring the width of the adjacent Holocene floodplain (see SM[1]). Reaches were defined as 'associated' with PCCS when the distance from the nearest bank was less than the mean channel width. For banks in each reach, we measured changes in water and land areas from 1984-2021 using the Global Surface Water Explorer (Pekel et al., 2016) to compute mean annual rates of erosion and deposition (see SM[1]).

RESULTS AND DISCUSSION

Bank Sediments and Strength

We find notable differences in composition between the left Holocene floodplain and the right PCCS. Left banks and islands are characterized by sandy bartop sediments (Figure 1B) often overlain by mud drapes, whereas the right banks are a heterogeneous succession with frequent outcrops of elevated PCCS (Figure 1C). The fine-grained PCCS materials are often lithified by ferruginous cements, iron and manganese crusts, and ferruginous coatings along vertical fractures (Rossetti et al., 2015; Pupim et al., 2019). Cliff collapses, marked by slump blocks comprising claystones interpreted as Pleistocene lacustrine sediments, expose large clay outcrops (Figure 1C).

These differences in deposits are reflected in our bank strength measurements: PCCS bank strength is variable, but on average up to three times greater than the Holocene deposits (SV;

Figure 2). PCCS containing sandy lenses exhibit values closer to those of the left bank. The CSM results reveal no significant difference between the resistant PCCS along the right bank and the Holocene deposits (Figure 2; SM[1]). Differences between these two datasets reflect that the CSM measures surface resuspension, related to hydraulic erosion processes, while the SV measures strength within a deeper surface layer, linked to mechanical bank failure (Tolhurst et al., 1999; He et al., 2018).

MBES and side-scan sonar images illustrate the prevalence of PCCS from bank top to toe (see also SM[1]), often extending far into the main channel (Figure 1D). These outcrops influence channel migration rates by locally reducing vertical and lateral erodibility, altering the flow dynamics, controlling the steering of bedload sediment, and providing local bank and bed protection. Such mechanisms have been highlighted in previous studies that have detailed the role of both near-bank bedrock (Nittrouer et al., 2011; Konsoer et al., 2016) and slump blocks associated with intermittent bank failures (Hackney et al., 2015). However, in those cases, bedrock outcrops were either located at the outer bank of sinuous channels or where channel curvature promoted deep scouring. PCCS outcrops documented herein are common along large stretches of the right bank of the Solimões River and the adjacent bed where channel curvature is low.

Reach- and System-Scale Dynamics

To assess the role of bank strength variability on erosion and deposition, we investigated three reaches classified as freely meandering or partially-constrained (Figure 3A). Figures 3B and 3C show an increasing asymmetry between erosion and deposition from reach I to III where PCCS were present (with the exception of B2). Bank erosion and deposition are balanced throughout reach I, where PCCS is absent and sinuosity is highest (1.33). Diminishing erosion along the right bank is linked to the presence of resistant layers in reach II (gray shades, Fig. 3C), where net bar deposition also decreases, indicating reduced bar formation and lower sinuosity (1.24). The main channel of reach III becomes stable when encountering the PCCS, which promotes reduced left bank erosion through low deposition and channel sinuosity (1.15). The secondary channel, which flows entirely along the resistant layers (see Figure 3A), remains stable along both banks with low erosion and deposition.

These trends illustrate that channel sinuosity and migration are strongly controlled by bank strength variability as recorded with the shear vane (Figure 3): high bank strength along one bank inhibits lateral erosion, which reduces local and downstream sediment availability, point bar deposition and steering of the flow. In the Amazon River, a substantial proportion of locally transported sediment originates from the floodplain, sourced through bank erosion and collapse (Dunne et al., 1998), which drives meandering through positive feedbacks between sediment flux and bar formation (Constantine et al., 2014). Such feedbacks are interrupted by the presence of PCCS that resist erosion and affect supply of bedload-sized material, evidenced by the absence of dunes near the PCCS banks (Figure 1D). The lack of bedforms implies that transport capacities exceed sediment supply for hundreds of meters from the bank, thus inhibiting bar deposition and maintaining channel position adjacent to the PCCS outcrops. The absence of flow steering due to lower channel curvature also stabilizes the left bank, despite the latter comprising more erodible alluvium. Resistance of the top sediment layer to failure (representative of the SV results) is likely to be the main control here compared to surface erosion processes. Although demanding future measurements of flow to test such reasoning, our observations provide a mechanistic link between the presence of PCCS and channel migration. Previous studies have suggested that changes in sinuosity and channel migration rates along the Solimões River are related to changes in slope and underlying geology (Dunne et al., 1998; Birkett et al., 2002; Dunne and Aalto, 2013). Our data show that bank strength is a primary control on differences in channel pattern in the Solimões River, with the stable right bank suppressing bank erosion and limiting creation of sinuous channels (Kleinhans et al., 2024), which thereby stabilizes both banks of the active channel.

Our GIS analysis over 1,600 km shows that the main channel frequently flows close to the higher terraces (Figure 4A, SM[1]), which are likely similar to the PCCS documented herein (Rossetti et al., 2015; Pupim et al., 2019). Reaches with the highest rates of erosion and deposition are disassociated from PCCS, whereas reaches associated with PCCS exhibit reduced erosion and deposition rates. PCCS therefore may influence larger scale dynamics in the Solimões River through the morphodynamic mechanisms proposed above, with possible implications for the controls on other large sand bed rivers where PCCS deposits have been reported, such as the Orinoco River (Meade et al., 1991), Late Holocene Willamette River (Wallick et al., 2022), Mekong River (Carling, 2009), and lower Mississippi River (Nittrouer et al., 2011).

CONCLUSIONS

A 100-km long reach of the Solimões River studied herein is characterized by Holocene floodplain deposits along its left bank and Pleistocene cohesive and cemented sediments (PCCS) along its right bank. Shear vane measurements show bank strength to be up to three times greater along the right as compared to the left bank. In reaches where PCCS are present, erosion and deposition rates are reduced, influencing channel sinuosity and migration. We argue that bar formation is suppressed along the right bank, due to limited channel widening and associated low sediment supply from the resistant PCCS. This reduced bar formation impedes steering of the flow and development of channel curvature, thereby lessening erosion of the weaker left bank towards the downstream. Migration analysis for the 1,600 km long river reveals that erosion and deposition decreases in reaches associated with PCCS, suggesting that these feedbacks affect sinuosity and lateral dynamics in the Solimões River, and potentially other large lowland rivers that possess significant PCCS.

ACKNOWLEDGMENTS

This project was funded by NERC grant NE/T007478/1. We thank Liliane Janikian Paes de Almeida, Felipe Figueiredo, Pedro Gomes and Carlos Manjon Mazoca for field support, USGS for the Corona imagery, RuralTech for the MBES survey, Planet Labs Inc. for satellite imagery, and Steve Darby for the CSM. Comments from Thomas Dunne and two anonymous reviewers significantly improved the manuscript.

REFERENCES

Ashworth, P.J., and Lewin, J., 2012, How do big rivers come to be different? Earth-Science Reviews, v. 114, p. 84–107, doi:10.1016/j.earscirev.2012.05.003.

Ashworth, P.J., Best, J.L., Roden, J., Bristow, C.S. and Klaassen, G.J. 2000, Morphological evolution and dynamics of a large, sand braid-bar, Jamuna River, Bangladesh, Sedimentology, 47, 533-555.

Birkett, C.M., Mertes, L.A.K., Dunne, T., Costa, M.H., and Jasinski, M.J., 2002, Surface water dynamics in the Amazon Basin: Application of satellite radar altimetry: Journal of Geophysical Research: Atmospheres, v. 107, p. 21–26, doi:10.1029/2001JD000609.

Boothroyd, R.J., Williams, R.D., Hoey, T.B., Barrett, B., and Prasojo, O.A., 2021, Applications of Google Earth Engine in fluvial geomorphology for detecting river channel change: Wiley Interdisciplinary Reviews: Water, v. 8, p. e21496, doi:10.1002/wat2.1496.

Carling, P.A., 2009, Geomorphology and Sedimentology of the Lower Mekong River, *in* The Mekong: Biophysical Environment of an International River Basin, Elsevier, p. 77–111, doi:10.1016/B978-0-12-374026-7.00005-X.

Constantine, J.A., Dunne, T., Ahmed, J., Legleiter, C., and Lazarus, E.D., 2014, Sediment supply as a driver of river meandering and floodplain evolution in the Amazon Basin: Nature Geoscience, v. 7, p. 899–903, doi:10.1038/ngeo2282.

Darby, S.E., and Thorne, C.R., 1996, Development and testing of riverbank-stability analysis: Journal of Hydraulic Engineering, v. 122, p. 443–454, doi:https://doi.org/10.1061/(ASCE)0733-9429(1996)122:8(443).

Dunne, T., and Aalto, R.E., 2013, Large River Floodplains, *in* Treatise on Geomorphology, Elsevier Inc., v. 9, p. 645–678, doi:10.1016/B978-0-12-374739-6.00258-X.

Dunne, T., Mertes, L.A.K., Meade, R.H., Richey, J.E., and Forsberg, B.R., 1998, Exchanges of sediment between the flood plain and channel of the Amazon River in Brazil: Bulletin of the Geological Society of America, v. 110, p. 450–467, doi:10.1130/0016-7606(1998)110<0450:EOSBTF>2.3.CO;2.

Güneralp, Í. and Rhoads, B.L., 2011, Influence of floodplain erosional heterogeneity on planform complexity of meandering rivers: Geophysical Research Letters, v. 38, doi:10.1029/2011GL048134.

Hackney, C., Best, J., Leyland, J., Darby, S.E., Parsons, D., Aalto, R., and Nicholas, A., 2015, Modulation of outer bank erosion by slump blocks: Disentangling the protective and destructive role of failed material on the three-dimensional flow structure: Geophysical Research Letters, v. 42, p. 10663–10670, doi:10.1002/2015GL066481.

Hawker, L., Uhe, P., Paulo, L., Sosa, J., Savage, J., Sampson, C., and Neal, J., 2022, A 30 m global map of elevation with forests and buildings removed: Environmental Research Letters, v. 17, doi:10.1088/1748-9326/ac4d4f.

He, C., You, Y., Wang, D., and Wu, H., 2018, Estimating soil failure due to torsion via vane shear test by varying vane diameter and soil properties: Soil and Tillage Research, v. 177, p. 68–78, doi:10.1016/j.still.2017.12.004.

Kleinhans, M.G., McMahon, W.J., and Davies, N.S., 2024, What even is a meandering river? A philosophy-enhanced synthesis of multi-level causes and systemic interactions contributing to river meandering: Geological Society, London, Special Publications, v. 540, p. SP540-2022, doi:10.1144/sp540-2022-138.

Konsoer, K.M., Rhoads, B.L., Langendoen, E.J., Best, J.L., Ursic, M.E., Abad, J.D., and Garcia, M.H., 2016, Spatial variability in bank resistance to erosion on a large meandering, mixed bedrock-alluvial river: Geomorphology, v. 252, p. 80–97, doi:10.1016/j.geomorph.2015.08.002.

Latrubesse, E.M., 2008, Patterns of anabranching channels: The ultimate end-member adjustment of mega rivers: Geomorphology, v. 101, p. 130–145, doi:10.1016/j.geomorph.2008.05.035.

Lehner, B., and Grill, G., 2013, Global river hydrography and network routing: Baseline data and new approaches to study the world's large river systems: Hydrological Processes, v. 27, p. 2171–2186, doi:10.1002/hyp.9740.

Maia, R.G.N., Godoy, H.K., de Moura, P.A., Ferreira da Costa, F.S., Arcanjo de Holanda, M., and de Alencar Costa, J., 1977, Projeto de carvão no alto Solimões. Relatório Final: CPRM-DNPM, p. 137.

Mertes, L.A.K., and Dunne, T., 2022, Effects of Tectonism and Sea-Level Change on the Form and Behaviour of the Modern Amazon River and Its Floodplain: Large Rivers: Geomorphology and Management, Second Edition, p. 171–204.

Mertes, L.A.K., Dunne, T., and Martinelli, L.A., 1996, Channel-floodplain geomorphology along the Solimões-Amazon River: GSA Bulletin, v. 108, p. 1089–1107, doi:https://doi.org/10.1130/0016-7606(1996)108<1089:CFGATS>2.3.CO;2.

Motta, D., Abad, J.D., Langendoen, E.J., and García, M.H., 2012, The effects of floodplain soil heterogeneity on meander planform shape: Water Resources Research, v. 48, doi:10.1029/2011WR011601.

Nittrouer, J.A., Mohrig, D., Allison, M.A., and Peyret, A.P.B., 2011, The lowermost Mississippi River: A mixed bedrock-alluvial channel: Sedimentology, v. 58, p. 1914–1934, doi:10.1111/j.1365-3091.2011.01245.x.

Parker, G., Shimizu, Y., Wilkerson, G. V., Eke, E.C., Abad, J.D., Lauer, J.W., Paola, C., Dietrich, W.E., and Voller, V.R., 2011, A new framework for modeling the migration of meandering rivers: Earth Surface Processes and Landforms, v. 36, p. 70–86, doi:10.1002/esp.2113

Pekel, J.F., Cottam, A., Gorelick, N., and Belward, A.S., 2016, High-resolution mapping of global surface water and its long-term changes: Nature, v. 540, p. 418–422, doi:10.1038/nature20584.

Planet, T., 2023, Planet application program interface: In space for life on Earth. San Francisco, CA.

Potter, E.P., 1978, Significance and Origin of Big Rivers: The Journal of Geology, v. 86, doi:https://doi.org/10.1086/649653.

Pupim, F.N. et al., 2019, Chronology of Terra Firme formation in Amazonian lowlands reveals a dynamic Quaternary landscape: Quaternary Science Reviews, v. 210, p. 154–163, doi:10.1016/j.quascirev.2019.03.008.

Rossetti, D.F. et al., 2015, Mid-Late Pleistocene OSL chronology in western Amazonia and implications for the transcontinental Amazon pathway: Sedimentary Geology, v. 330, p. 1–15, doi:10.1016/j.sedgeo.2015.10.001.

Schwendel, A.C., Nicholas, A.P., Aalto, R.E., Sambrook Smith, G.H., and Buckley, S., 2015, Interaction between meander dynamics and floodplain heterogeneity in a large tropical sand-bed river: The Rio Beni, Bolivian Amazon: Earth Surface Processes and Landforms, v. 40, p. 2026–2040, doi:10.1002/esp.3777.

Schwenk, J., Khandelwal, A., Fratkin, M., Kumar, V., and Foufoula-Georgiou, E., 2017, High spatiotemporal resolution of river planform dynamics from Landsat: The rivMAP toolbox and results from the Ucayali River: Earth and Space Science, v. 4, p. 46–75, doi:10.1002/2016EA000196.

Tolhurst, T.J., Black, K.S., Shayler, S.A., Mather, S., Black, I., Baker, K., and Paterson, D.M., 1999, Measuring the in situ Erosion Shear Stress of Intertidal Sediments with the Cohesive Strength Meter (CSM): Estuarine, Coastal and Shelf Science, v. 49, p. 281–294, doi:https://doi.org/10.1006/ecss.1999.0512.

van de Lageweg, W.I., van Dijk, W.M., Baar, A.W., Rutten, J., and Kleinhans, M.G., 2014, Bank pull or bar push: What drives scroll-bar formation in meandering rivers? Geology, v. 42, p. 319–322, doi:10.1130/G35192.1.

Wallick, J.R., Grant, G., Lancaster, S., Bolte, J.P., and Denlinger, R., 2022, Patterns and controls on historical channel change in the Willamette River, Oregon USA: Large Rivers: Geomorphology and Management, Second Edition, p. 737–775.

Zhao, K., Coco, G., Gong, Z., Darby, S.E., Lanzoni, S., Xu, F., Zhang, K., and Townend, I., 2022, A Review on Bank Retreat: Mechanisms, Observations, and Modeling: Reviews of Geophysics, v. 60, p. 1–51, doi:10.1029/2021rg000761.

[1]Supplementary Material provides measurements, GIS data, and Landsat, Corona, and MBES imagery (https://doi.org/10.1130/XXXX).

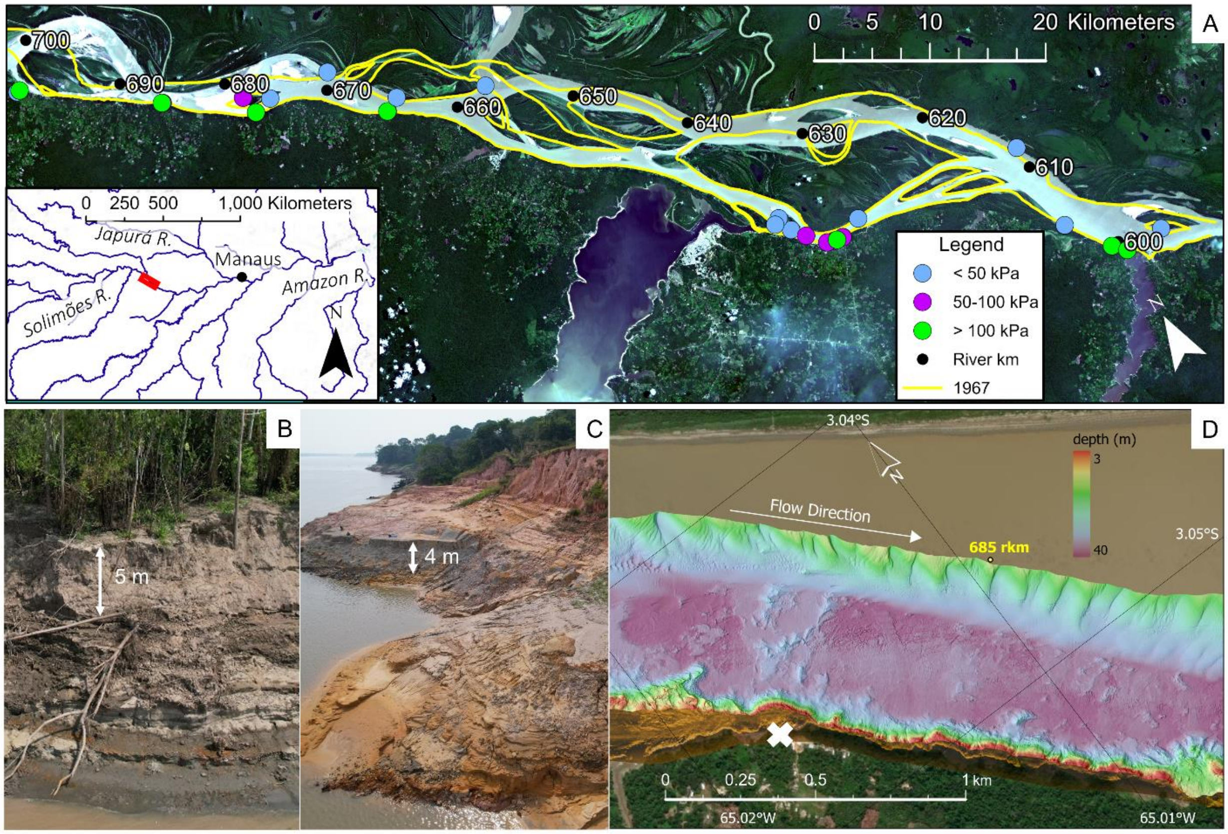

Figure 1. A: Study area with bank and bar lines from 1967 (Corona; yellow lines) superimposed on 2021 (PlanetScope) imagery, showing varying migration rates between left and right bank. Colored points denote measurement locations along the 100-km reach of the Solimões River of three strength classes obtained with the shear vane. Inset map shows the river network (HydroSHEDS; Lehner and Grill, 2013) and study site location in the Amazon River Basin (red rectangle). B: Photograph of Holocene deposits on the left bank; C: Photograph of Pleistocene mud- and sandstones on the right bank. D: Multibeam echo sounder and side-scan (< 3 m; marked by an X) data showing PCCS outcrops along the right bank and extending across the channel, with the margins of large sand dunes in the channel center.

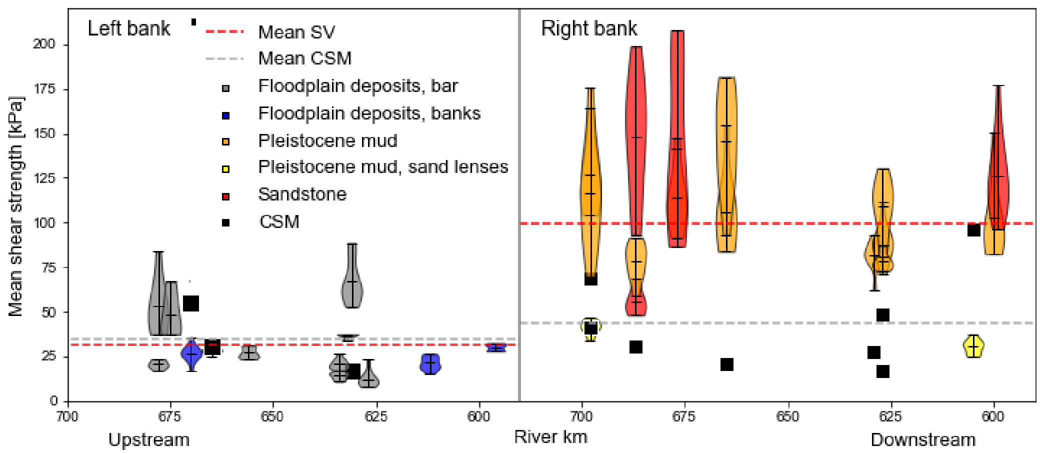

Figure 2. Bank strength measurements along the 100-km reach of the Solimões River (see Figure 1A for location). Violin plots represent mean, 25th-, and 75th-percentiles measured by the shear vane (SV). Colors indicate lithological characteristics of the samples, with black squares showing results from the cohesion strength meter (CSM) multiplied by a factor of 10,000 to aid visibility. t-tests reveal a significant difference between mean bank strengths at the left and right banks for the SV measurements (p-value < 0.05), but not for the CSM (p-value > 0.05) (see SM[1]).

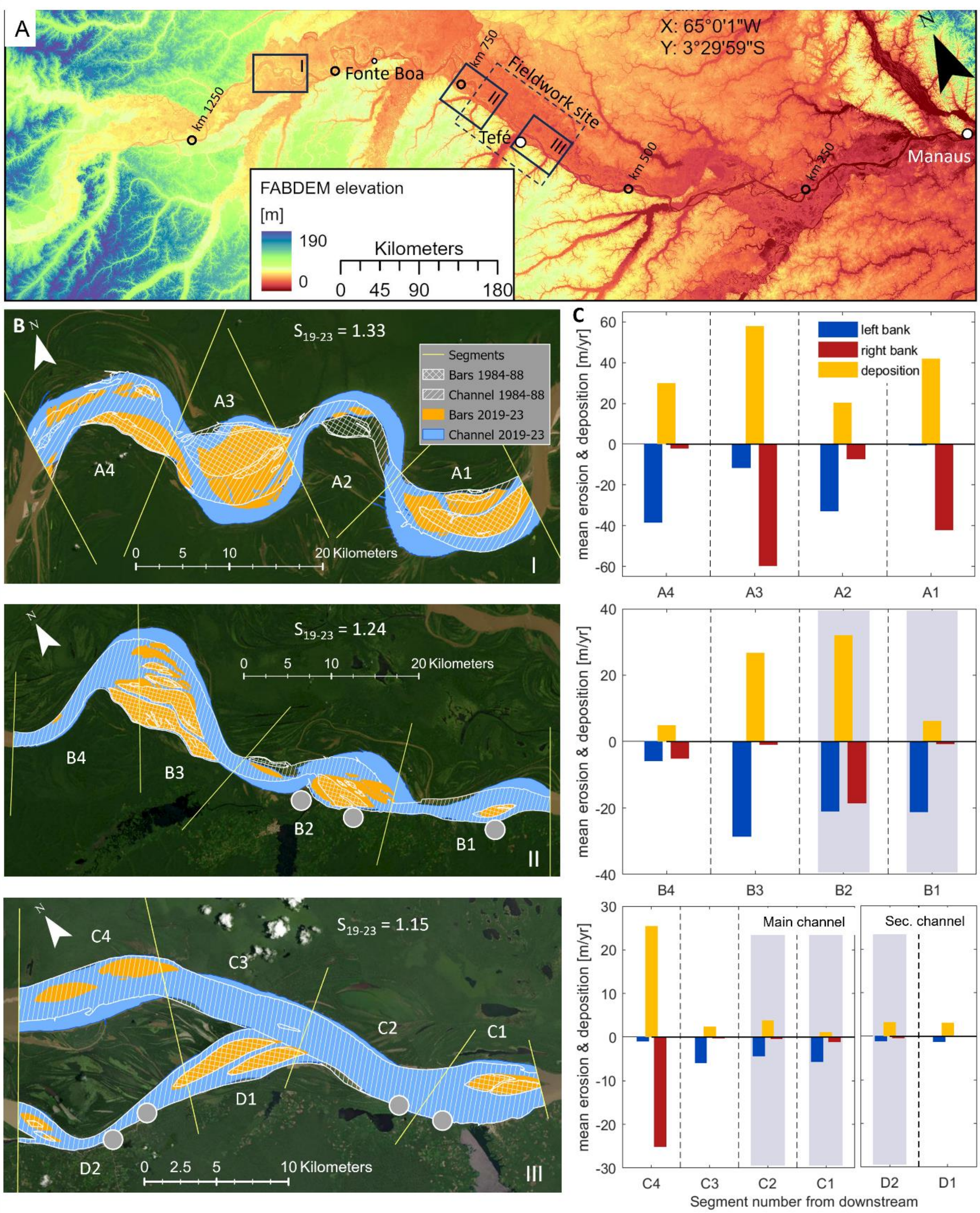

Figure 3. A. Digital elevation model of the Solimões River with locations of (I) a freely meandering reach (river km 1040-1120), (II) a partially-constrained reach (river km 670-750);

and (III) a partially-constrained reach at the confluence with a secondary channel (river km 590-630). Fieldwork site is indicated (dashed rectangle). B. Overlays of channel and bar area averaged between 1984-1988 (white hatched areas) and 2019-2023 (blue and orange areas) derived from Landsat imagery. Yellow lines indicate segments of *c.* 20 km (reaches I and II) and 10 km (reach III) width; gray circles denote locations of measured resistant layers. C. Bank erosion along each bank, and net deposition averaged over each segment, compared to locations of the resistant layers (SV > 100 kPa) observed in the field marked as gray shades.

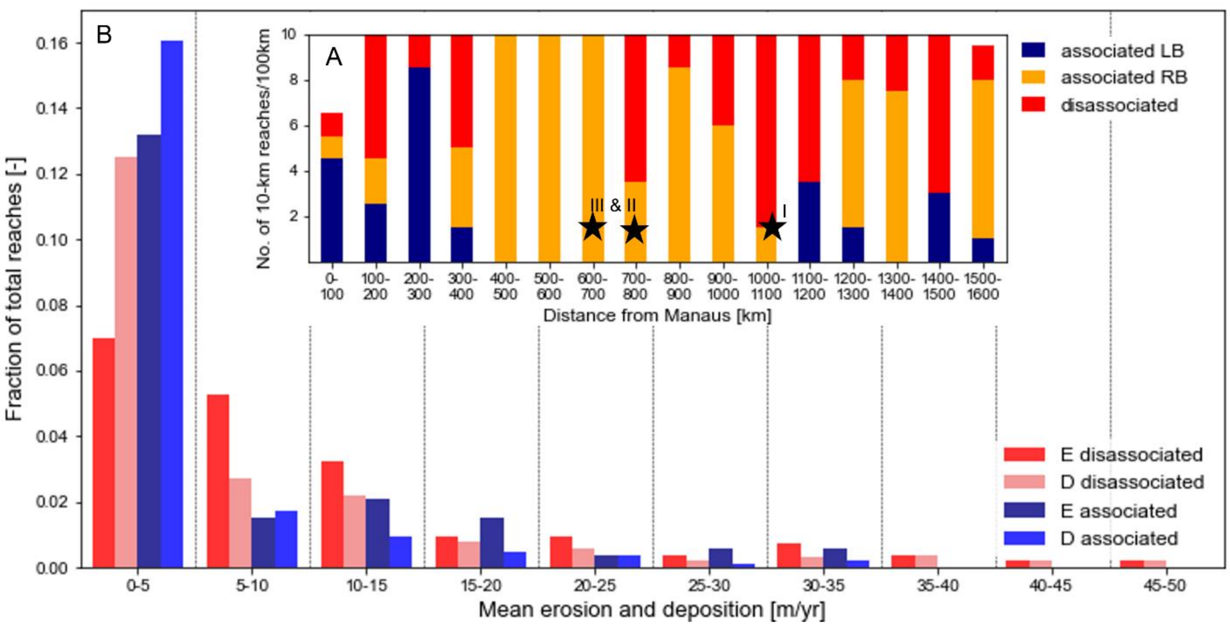

Figure 4. (A) Number of reaches classified as associated and disassociated with PCCS with distance from Manaus. Reaches in the present study are marked as stars for context. (B) Fraction of associated and disassociated reaches over mean erosion (E) and deposition (D) rate. Two-sample Kolmogorov-Smirnoff Test for erosion and deposition show significantly different distributions (p-values < 0.05) (see SM[1]).